THEORETICAL & APPLIED MECHANICS LETTERS **2**, 043004 (2012)

Stability case study of the ACROBOTER underactuated service robot

László L. Kovács,[1, a)] and László Bencsik[2, b)]
[1)] *HAS-BME Research Group on Dynamics of Machines and Vehicles, Budapest H-1521, Hungary*
[2)] *Department of Applied Mechanics, Budapest University of Technology and Economics, Budapest H-1521, Hungary*

(Received 10 June 2012; accepted 20 June 2012; published online 10 July 2012)

Abstract The dynamics of classical robotic systems are usually described by ordinary differential equations via selecting a minimum set of independent generalized coordinates. However, different parameterizations and the use of a nonminimum set of (dependent) generalized coordinates can be advantageous in such cases when the modeled device contains closed kinematic loops and/or it has a complex structure. On one hand, the use of dependent coordinates, like natural coordinates, leads to a different mathematical representation where the equations of motion are given in the form of differential algebraic equations. On the other hand, the control design of underactuated robots usually relies on partial feedback linearization based techniques which are exclusively developed for systems modeled by independent coordinates. In this paper, we propose a different control algorithm formulated by using dependent coordinates. The applied computed torque controller is realized via introducing actuator constraints that complement the kinematic constraints which are used to describe the dynamics of the investigated service robotic system in relatively simple and compact form. The proposed controller is applied to the computed torque control of the planar model of the ACROBOTER service robot. The stability analysis of the digitally controlled underactuated service robot is provided as a real parameter case study for selecting the optimal control gains. [doi:10.1063/2.1204304]

Keywords stability, underactuation, natural coordinates, control constraints

In case of complex multibody problems or closed loop manipulators, geometric constraint conditions have to be considered during dynamics modeling and simulation. These systems are often described by a dependent set of generalized coordinates subjected to constraints that provide an efficient formalism to generate the equations of motion in the form of differential algebraic equations (DAE).

When a contact is established, an interaction force will develop between the multibody system and its environment at the point of contact. The corresponding generalized force can be interpreted as a result of specifying certain conditions or restraints on the motion in the constrained direction.[1] Another important use of constraints in modeling dynamical system is defining certain rigid body and interconnection-type assumption to simplify the representation of complex multibody systems. In this context, Ref. 2 discusses the possible advantages of using a special set of dependent coordinates, the so-called natural coordinates, in the real-time dynamic simulation of mechanical systems. In addition, servo constraints (also called as control or actuator constraints) form an important class of constraints. Unlike their physical (or passive) counterparts, they are used to define a prescribed path problem and therefore servo constraints are rather part of the performance specifications.[3,4]

Control methods for underactuated manipulators, such as partial feedback linearization (PFL)[5] and the computed desired computed torque control (CDCTC) method[6] are mainly developed for systems described by independent coordinates. The PFL can be used to feedback linearize the dynamics corresponding to the active degrees of freedom, and in case of strong inertial coupling the dynamics corresponding to the passive degrees of freedom of a system. In connection with the categories of active and passive coordinates, Ref. 6 introduces controlled and uncontrolled coordinates. While the controlled coordinates are prescribed, the trajectories of the uncontrolled coordinates are calculated online which makes the error feedback possible for all degrees of freedom. The on-line calculation of these coordinates requires the solution of the equation of motion projected into the space of uncontrolled motion. Following the same idea, Ref. 7 presents a computed torque based solution for the position control of a suspended service robot ACROBOTER[8] that is modeled by dependent coordinates. In that study, the desired values of the uncontrolled coordinates and the control input are determined via the direct solution of the DAE equations of motion discretized via the backward Euler method.

By making use of the concept of servo-constraints, here, a computationally more effective computed torque control strategy is proposed based on the method of Lagrangian multipliers combined with a proportional derivative (PD) controller for enforcing the servo-constraints. The problem is formulated in dependent coordinates which yiels both geomterical and servo-constraints imposed on the robot dynamics. The applied control provides similar constraint stabilization for the servo-constraints as the Baumgarte stabilization[9] for the passive geomteric constraints. Advantages of

[a)] Email: kovacs@mm.bme.hu.
[b)] Corresponding author. Email: bencsik@mm.bme.hu.

using dependent coordinates to formulate control problems of underactuated systems are also demonstrated in Ref. 10. The recent work presents the application of the proposed computed torque control strategy to the planar model of the ACROBOTER system. The DAE equations of motion are linearized around the typical working configuration of the robot and the optimal control parameters are determined via detailed stability analysis.

It is assumed that the dynamics of the studied underactuated system is modeled by using dependent coordinates resulting in the equation of motion

$$\boldsymbol{M}\ddot{\boldsymbol{q}} + \boldsymbol{\Phi}_{\boldsymbol{q}}^{\mathrm{T}}\boldsymbol{\lambda} = \boldsymbol{Q} + \boldsymbol{H}\boldsymbol{u}\,, \tag{1}$$

$$\boldsymbol{\phi}_g = \boldsymbol{0}, \tag{2}$$

where $\boldsymbol{M}(\boldsymbol{q}) \in \mathbb{R}^{n\times n}$ is the mass matrix, $\boldsymbol{\Phi}(\boldsymbol{q}) \in \mathbb{R}^{m\times n}$ is the Jacobian of geometric constraints $\boldsymbol{\phi}_g(\boldsymbol{q}, t) \in \mathbb{R}^m$ and $\boldsymbol{\lambda} \in \mathbb{R}^m$ is the vector of the Lagrangian multipliers. Matrix $\boldsymbol{H}(\boldsymbol{q}) \in \mathbb{R}^{n\times l}$ is the control input matrix and $\boldsymbol{u} \in \mathbb{R}^l$ contains the actuating forces and torques. In addition, $\boldsymbol{Q}(\boldsymbol{q}, \dot{\boldsymbol{q}}) \in \mathbb{R}^n$ denotes the remaining generalized forces like the gravity and/or the Coriolis and centrifugal terms. The system described by Eqs. (1) and (2) has $r = n - m$ degrees of freedom. The number of actuating forces l is such that $l < r$ providing that the system is underactuated.

For the sake of simplicity, in the following derivations, we assume that the geometric constraints do not have components with explicit time dependence. Thus, the constraints at the acceleration level has the form

$$\ddot{\boldsymbol{\phi}}_g = \boldsymbol{\Phi}_{\boldsymbol{q}}\ddot{\boldsymbol{q}} + \dot{\boldsymbol{\Phi}}_{\boldsymbol{q}}\dot{\boldsymbol{q}}\,. \tag{3}$$

An important element of the presented approach is the use of the concept of servo-constraints[4] specifying the desired motion of the constrained system as function of the generalized coordinates and time. The servo constraint equations are formulated similar to the geometric ones, but they involve control specification terms that may depend on time explicitly. It is assumed that the number of the servo-constraints is equal to the number l of actuating forces. These constraints are represented at the position and acceleration level by

$$\boldsymbol{\phi}_{\mathrm{s}}(\boldsymbol{q}, t) = \boldsymbol{0}, \quad \ddot{\boldsymbol{\phi}}_{\mathrm{s}} = \boldsymbol{G}_{\boldsymbol{q}}\ddot{\boldsymbol{q}} + \dot{\boldsymbol{G}}_{\boldsymbol{q}}\dot{\boldsymbol{q}} + \dot{\boldsymbol{c}}, \tag{4}$$

where

$$\boldsymbol{G}_{\boldsymbol{q}} = \frac{\partial \boldsymbol{\phi}_{\mathrm{s}}}{\partial \boldsymbol{q}}, \quad \boldsymbol{c} = \frac{\partial \boldsymbol{\phi}_{\mathrm{s}}}{\partial t}\,.$$

Combining the equation of motion (1) and the kinematic- and the servo-constraints (3) and (4) at the acceleration level, similarly to the method of Lagrange multipliers, the accelerations $\ddot{\boldsymbol{q}}$, the Lagrange multipliers $\boldsymbol{\lambda}$ and the control input $\boldsymbol{u}$ can be calculated as the solution of the system

$$\begin{bmatrix} \boldsymbol{M} & \boldsymbol{\Phi}_{\boldsymbol{q}}^{\mathrm{T}} & -\boldsymbol{H} \\ \boldsymbol{\Phi}_{\boldsymbol{q}} & \boldsymbol{0} & \boldsymbol{0} \\ \boldsymbol{G}_{\boldsymbol{q}} & \boldsymbol{0} & \boldsymbol{0} \end{bmatrix} \begin{bmatrix} \ddot{\boldsymbol{q}} \\ \boldsymbol{\lambda} \\ \boldsymbol{u} \end{bmatrix} = \begin{bmatrix} \boldsymbol{Q} \\ -\dot{\boldsymbol{\Phi}}_{\boldsymbol{q}}\dot{\boldsymbol{q}} \\ -\dot{\boldsymbol{G}}_{\boldsymbol{q}}\dot{\boldsymbol{q}} - \dot{\boldsymbol{c}} - k_{\mathrm{D}}\dot{\boldsymbol{\phi}}_{\mathrm{s}} - k_{\mathrm{P}}\boldsymbol{\phi}_{\mathrm{s}} \end{bmatrix}, \tag{5}$$

where the control gains k_{P} and k_{D} play a similar role as the Baumgarte parameters[9] in the solution of DAE equations of motion. When there are only geometric constraints, the Baumgarte parameters are used to stabilize those constraints. Here, the control parameters k_{P} and k_{D} are to realize a PD controller that enforces the servo-constraints through which the desired motion of the system is defined. Assuming that the state of the system is measured and the leading matrix of Eq. (5) is invertible, the necessary control action can be calculated. The geometric constraints have to be independent to ensure the invertability. Applying only the servo-constraints, the invertability depends on the rank of the matrix $\boldsymbol{G}_{\boldsymbol{q}}\boldsymbol{M}^{-1}\boldsymbol{H}$. For further details on the realization of the servo-constraints, readers can refer to Ref. 3. With the above assumptions the proposed controller will be applied for a novel service robot described as follows.

The ACROBOTER platform is a service robot that crawls in the plane of the ceiling and has a pendulum-like working unit.[8] The different subsystems of this robot are shown in Fig. 1.

The system of anchor points is placed on the ceiling in a triangular grid. The climbing unit (CU), which is a planar RRT robot, can move by grasping these anchor points. The swinging unit (SU) is connected to the climbing unit via a main and three subsequent orienting cables. These four cables are fixed in one point by the cable connector (CC). The horizontal motion of the SU is mainly provided by the climbing unit, while in the vertical direction it is elevated by the main cable. In addition, the SU has ducted fan actuators that contribute to the control of the horizontal motion. The cable connector has no actuators (like the ducted fans of the SU) and therefore its position cannot directly be controlled. Consequently the ACROBOTER platform is underactuated and typically the motion of the CC parallel to the plane of the base plate of the SU is determined via the internal dynamics of the system.

For analyzing the stability of the proposed controller applied to the ACROBOTER robot a representative planar model is constructed (see right in Fig. 1). In this model the swinging unit is modeled as a planar rigid body and the cable connector is simply represented as a point mass. The connecting windable cables are considered as ideal cables. In case of the recent prototype the climbing unit has an independent position controller and only used to carry the swinging unit. Thus, considering slow motion of the CU, the system can be described by a model with fixed hoisting point.

To describe the geometry of the model in Fig. 1 the most convenient is to use the fully Cartesian coordinates $\boldsymbol{q} = [x_2\ y_2\ x_3\ y_3\ x_4\ y_4]^{\mathrm{T}}$, where the last four elements are the so-called natural coordinates that belong to the planar rigid body that represents the SU. Thus, according to Ref. 2, the mass matrix of the planar

ACROBOTER model can be assembled as a constant block diagonal matrix $\boldsymbol{M} = \mathrm{diag}(\boldsymbol{M}_{\mathrm{CC}}\ \boldsymbol{M}_{\mathrm{SU}})$ with the blocks $\boldsymbol{M}_{\mathrm{CC}} = m_{\mathrm{CC}}\,\boldsymbol{I}$, where $\boldsymbol{I}$ is the 2 by 2 identity matrix, and

$$\boldsymbol{M}_{\mathrm{SU}} = \begin{bmatrix} \frac{m_{\mathrm{SU}}(L-2\xi_{\mathrm{CM}})}{L} + \frac{J}{L^2} & 0 & \frac{m_{\mathrm{SU}}\xi_{\mathrm{CM}}}{L} - \frac{J}{L^2} & -\frac{m_{\mathrm{SU}}\eta_{\mathrm{CM}}}{L} \\ 0 & \frac{m_{\mathrm{SU}}(L-2\xi_{\mathrm{CM}})}{L} + \frac{J}{L^2} & \frac{m_{\mathrm{SU}}\eta_{\mathrm{CM}}}{L} & \frac{m_{\mathrm{SU}}\xi_{\mathrm{CM}}}{L} - \frac{J}{L^2} \\ \frac{m_{\mathrm{SU}}\xi_{\mathrm{CM}}}{L} - \frac{J}{L^2} & \frac{m_{\mathrm{SU}}\eta_{\mathrm{CM}}}{L} & \frac{J}{L^2} & 0 \\ -\frac{m_{\mathrm{SU}}\eta_{\mathrm{CM}}}{L} & \frac{m_{\mathrm{SU}}\xi_{\mathrm{CM}}}{L} - \frac{J}{L^2} & 0 & \frac{J}{L^2} \end{bmatrix}, \tag{6}$$

where L is the distance between the basic points P_3 and P_4, m_{CC} and m_{SU} are the masses of the CC and SU, respectively, and J is the mass moment of inertia of the SU with respect to point P_3. In addition, ξ_{CM} and η_{CM} give the location of the center of mass of the SU in the body fixed frame $\{P_3; \xi, \eta, \zeta\}$.

The dependent coordinates are subjected to the kinematic constraint

$$\boldsymbol{\phi}_g = \frac{1}{2}\left[(x_3 - x_4)^2 + (y_3 - y_4)^2 - L^2\right] = 0\,, \tag{7}$$

where the selection of the quadratic constraint expression leads to a constraint Jacobian which is linear in terms of the dependent coordinates

$$\boldsymbol{\Phi}_{\boldsymbol{q}} = [0\ \ 0\ \ x_3 - x_4\ \ y_3 - y_4\ \ x_4 - x_3\ \ y_4 - y_3]\,. \tag{8}$$

The system of applied forces consist of the gravity force and the control forces. Using the natural coordinate representation the gravity force has the simple constant form

$$\boldsymbol{Q}_g = \Big[0\ \ -m_{\mathrm{CC}}g\ \ \frac{m_{\mathrm{SU}}g\eta_{\mathrm{CM}}}{L}\ \ \frac{m_{\mathrm{SU}}g(\xi_{\mathrm{CM}} - L)}{L}\ \ -\ \ \frac{m_{\mathrm{SU}}g\eta_{\mathrm{CM}}}{L}\ \ -\frac{m_{\mathrm{SU}}g\xi_{\mathrm{CM}}}{L}\Big]^{\mathrm{T}}. \tag{9}$$

The control forces are collected in the vector $\boldsymbol{u} = [F_1\ F_2\ F_3\ F_{\mathrm{T}}]^{\mathrm{T}}$, where F_1 is the tension in the main cable, F_2 and F_3 are the cable forces applied through the orienting cables and F_{T} is the thrust force provided by the ducted fan actuator. The point of action of the thrust force is given by the parameters ξ_{T} and η_{T} in the body fixed frame. With this, the applied control forces can be expressed by the term $\boldsymbol{H}\boldsymbol{u}$, where the control input matrix $\boldsymbol{H}$ has the form

$$\boldsymbol{H} = \begin{bmatrix} -\frac{x_2}{l_1} & \frac{x_3 - x_2}{l_2} & \frac{x_4 - x_2}{l_3} & 0 \\ -\frac{y_2}{l_1} & \frac{y_3 - y_2}{l_2} & \frac{y_4 - y_2}{l_3} & 0 \\ 0 & \frac{x_2 - x_3}{l_2} & 0 & \frac{(\xi_{\mathrm{T}} - L)x_3 + (L - \xi_{\mathrm{T}})x_4 + \eta_{\mathrm{T}}(y_3 - y_4)}{L^2} \\ 0 & \frac{y_2 - y_3}{l_2} & 0 & \frac{\eta_{\mathrm{T}}x_4 - \eta_{\mathrm{T}}x_3 - (L - \xi_{\mathrm{T}})(y_3 - y_4)}{L^2} \\ 0 & 0 & \frac{x_2 - x_4}{l_3} & \frac{\xi_{\mathrm{T}}x_4 - \xi_{\mathrm{T}}x_3 + \eta_{\mathrm{T}}(y_4 - y_3)}{L^2} \\ 0 & 0 & \frac{x_2 - x_4}{l_3} & \frac{\eta_{\mathrm{T}}x_3 - \eta_{\mathrm{T}}x_4 - \xi_{\mathrm{T}}y_3 + \xi_{\mathrm{T}}y_4}{L^2} \end{bmatrix}, \tag{10}$$

and l_i, $i = 1, 2, 3$ denote the changing lengths of the main and the orienting cables. These lengths can conveniently be expressed as functions of the dependent coordinates.

The typical control task of the ACROBOTER robot is to follow a desired trajectory such that the climbing unit is above the swinging unit the horizontal orientation of which is maintained by the orienting cables. The thrust force is used to accelerate or decelerate the SU as well as to react to horizontal perturbations. Thus for the stability analysis we consider that the SU is horizontal and its center of mass is below the suspension point. In this hanging down position the linearized dynamics of the uncontrolled system will become decoupled in

the x and y directions. Therefore, the applied controller must establish some coupling between the dynamics of the SU and the CC in order to provide sufficient damping for the (uncontrolled) horizontal vibrations of the cable connector.

In the following, providing that the SU is horizontal, the desired configuration of the system is given by the constants $x^{\mathrm{d}}_{\mathrm{CM}}$, $y^{\mathrm{d}}_{\mathrm{CM}}$ and $h^{\mathrm{d}}_{\mathrm{CC}}$, where $(x^{\mathrm{d}}_{\mathrm{CM}}, y^{\mathrm{d}}_{\mathrm{CM}})$ is the desired position of the SU and $h^{\mathrm{d}}_{\mathrm{CC}}$ is the desired elevation of the CC above the SU. For the sake of simplicity, we also assume that the center of mass of the planar model is in the middle of the representing rod, i.e., $\xi_{\mathrm{CM}} = L/2$ and $\eta_{\mathrm{CM}} = 0$ (see Fig. 1). With these notations, the servo-constraints associated with the control task can be written in the linear form

$$\boldsymbol{\phi}_{\mathrm{s}} = \begin{bmatrix} y_{\mathrm{CC}} - \dfrac{y_3 + y_4}{2} - h^{\mathrm{d}}_{\mathrm{CC}} \\ (1-\gamma)x_2 + \gamma\dfrac{x_3 + x_4}{2} - x^{\mathrm{d}}_{\mathrm{CM}} \\ \dfrac{y_3 + y_4}{2} - y^{\mathrm{d}}_{\mathrm{CM}} \\ y_3 - y_4 \end{bmatrix}, \tag{11}$$

where factor γ is used to couple the dynamics of the CC and the SU.

In order to investigate the stability of the digitally controlled system around a desired equilibrium position the equation of motion as well as the constraint equations have to be linearized around that position (configuration).

A few study exist where the direct linearization of the constrained multibody dynamic equations are used to analyze the stability and dynamical characteristics, such as vibration frequencies, of complex and large deformable mechanical systems.[11,12] In these works, the Lagrangian multipliers associated with the constraints are considered as variables in a generalized eigenvalue problem that, beside the physically meaningful ones, results in spurious eigenvalues which do not characterize the dynamics of the investigated system. Reference 12 describes how these eigenvalues result from the algebraic part of the problem and how they can be recognized and isolated. Another, and the most common, technique for the linearization of the DAE equations of motion is the elimination of the algebraic constraint equations by means of an orthogonal projection[13] and linearizing the resulting set of equations which are depend only on the selected minimum set of coordinates.

As a third alternative, one can linearize the original set of DAE equations, which is followed by an orthogonal projection in order to provide the linearized equation of motion in an appropriate form for the stability analysis.[14] By following this procedure, let $\boldsymbol{p} = [x_{\mathrm{CC}}\ y_{\mathrm{CC}}\ x_{\mathrm{CM}}\ y_{\mathrm{CM}}\ \theta]^{\mathrm{T}}$ denote the minimum set of generalized coordinates where the subscripts CC and CM refers to the cable connector and the center of mass of the SU, respectively, and θ represents the pitch of the swinging unit. These coordinates can be introduced via the transformation $\dot{\boldsymbol{q}} = \boldsymbol{R}\dot{\boldsymbol{p}}$ where the Jacobian matrix of the transformation is

$$\boldsymbol{R} = \begin{bmatrix} 1 & 0 & 0 & 0 & 0 \\ 0 & 1 & 0 & 0 & 0 \\ 0 & 0 & 1 & 0 & \dfrac{L}{2}\sin\theta - \eta_{\mathrm{CM}}\cos\theta \\ 0 & 0 & 0 & 1 & -\dfrac{L}{2}\cos\theta - \eta_{\mathrm{CM}}\sin\theta \\ 0 & 0 & 1 & 0 & -\dfrac{L}{2}\sin\theta - \eta_{\mathrm{CM}}\cos\theta \\ 0 & 0 & 0 & 1 & \dfrac{L}{2}\cos\theta - \eta_{\mathrm{CM}}\sin\theta \end{bmatrix}. \tag{12}$$

Then the linearized equations of motion in terms of the independent generalized coordinates reads

$$\boldsymbol{R}_0^{\mathrm{T}}\boldsymbol{M}\boldsymbol{R}_0\,\delta\ddot{\boldsymbol{p}} + \boldsymbol{R}_0^{\mathrm{T}}\left(\frac{\partial\boldsymbol{\Phi}^{\mathrm{T}}\boldsymbol{\lambda}}{\partial\boldsymbol{q}} - \frac{\partial\boldsymbol{H}u}{\partial\boldsymbol{q}}\right)_0\boldsymbol{R}_0\,\delta\boldsymbol{p} = \boldsymbol{R}_0^{\mathrm{T}}\boldsymbol{H}_0\,\delta\boldsymbol{u}\,, \tag{13}$$

where δ denotes the small perturbation of the prefixed quantity and the subscript zero refers to the desired equilibrium. By denoting the linearized mass, stiffness and control input matrices with $\widetilde{\boldsymbol{M}}$, $\widetilde{\boldsymbol{K}}$ and $\widetilde{\boldsymbol{H}}$, respectively, the equations of motion of the digitally controlled system can finally be written in the compact form

$$\widetilde{\boldsymbol{M}}\,\delta\ddot{\boldsymbol{p}} + \widetilde{\boldsymbol{K}}\,\delta\boldsymbol{p} = \widetilde{\boldsymbol{H}}\,\delta\boldsymbol{u}_{j-1}, \quad t \in [t_j, t_j + \Delta t), \tag{14}$$

where $\boldsymbol{u}_{j-1}$ is the constant control action applied during the jth sampling interval. In the applied sampling model we assume uniform sampling with sampling time Δt and a unit delay followed by a zero order hold.

The linearized equation of motion (14) is augmented by the linearized servo-constraints

$$\boldsymbol{\phi}_{\mathrm{s}} = \begin{bmatrix} y_{\mathrm{CC}} - y_{\mathrm{SU}} - h^{\mathrm{d}}_{\mathrm{CC}} \\ (1-\gamma)x_{\mathrm{CC}} + \gamma x_{\mathrm{SU}} - x^{\mathrm{d}}_{\mathrm{CM}} \\ y_{\mathrm{SU}} - y^{\mathrm{d}}_{\mathrm{CM}} \\ -L\theta \end{bmatrix}, \tag{15}$$

which implicitly defines the actuator forces.

Considering full state feedback, the applied control forces $\delta\boldsymbol{u}_{j-1}$ can be expressed via the solution of the system (14) and (15) at the corresponding sampling instant $t_{j-1} = (j-1)\Delta t$. By using this solution, the linearized equations of motion can be represented in the state space form $\dot{\boldsymbol{x}} = \boldsymbol{A}\boldsymbol{x} + \boldsymbol{B}\boldsymbol{x}_{j-1}$ with $\boldsymbol{x} = [\boldsymbol{p}\ \dot{\boldsymbol{p}}]^{\mathrm{T}}$, where we assume that the generalized velocity components are available as measured signals. The solution for the next sample value is then given by $\boldsymbol{x}_{j+1} = \boldsymbol{A}_{\mathrm{d}}\boldsymbol{x}_j + \boldsymbol{B}_{\mathrm{d}}\boldsymbol{x}_{j-1}$ with $\boldsymbol{A}_{\mathrm{d}} = \mathrm{e}^{\boldsymbol{A}\Delta t}$ and $\boldsymbol{B}_{\mathrm{d}} = \int_0^{\Delta t}\mathrm{e}^{\boldsymbol{A}\tau}\,\mathrm{d}\,\tau$.[15] Note, that the solution corresponding to the inhomogeneous part cannot be expressed by using the inverse of the system matrix $\boldsymbol{A}$ since this matrix is singular in the linearized case. The corresponding zero eigenvalue refers to the translational motion of the linearized system in the y direction.

Then by introducing the new discrete state variable $\boldsymbol{z}_j = [\boldsymbol{x}_j\ \boldsymbol{x}_{j-1}]^{\mathrm{T}}$ the stability of the digitally controlled

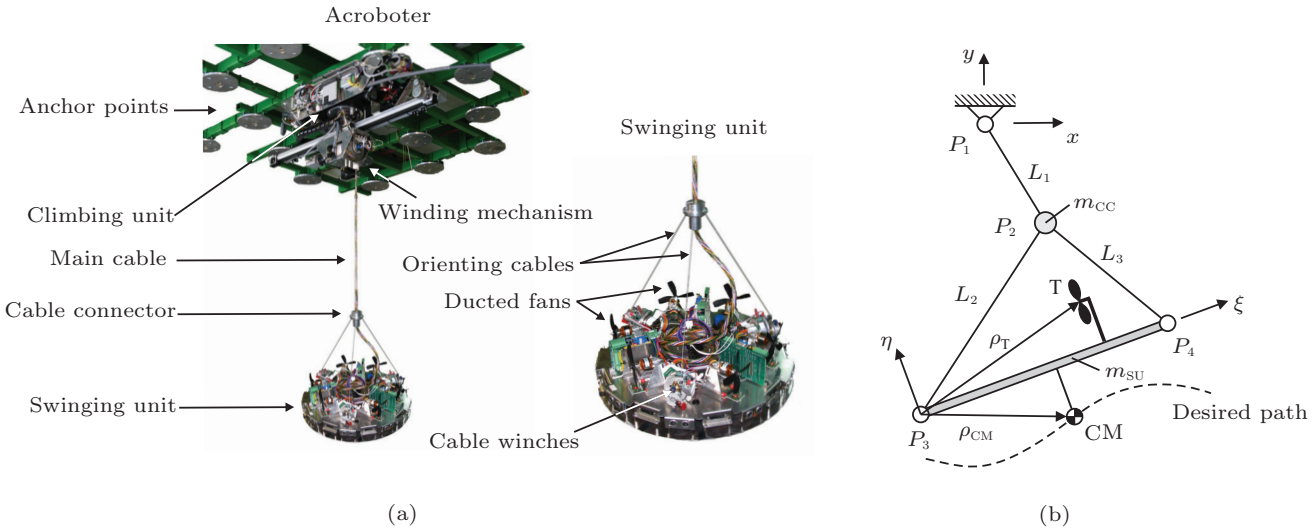

Fig. 1. The ACROBOTER robot (a) and its planar model (b).

Table 1. Model parameters.

m_{CC}	m_{SU}	J	Δt	ξ_{SU}	η_{SU}	ξ_T	η_T
0.1 kg	5 kg	0.4 kg/m^2	0.01 s	0.25 m	0 m	0.25 m	0.05 m

system can be investigated by calculating the eigenvalues of the discrete mapping constructed from the piecewise solution of the equation of motion[15]

$$\boldsymbol{z}_{j+1} = \boldsymbol{W}\boldsymbol{z}_j \quad \text{with} \quad \boldsymbol{W} = \begin{bmatrix} \boldsymbol{A}_d & \boldsymbol{B}_d \\ \boldsymbol{I} & \boldsymbol{0} \end{bmatrix}. \tag{16}$$

The convergence of the multi dimensional geometric series $\boldsymbol{z}_{j+1} = \boldsymbol{W}\boldsymbol{z}_j$ in Eq. (16) is equivalent to the asymptotic stability of the desired motion of the controlled system. Thus, to ensure stability, the eigenvalues of $\boldsymbol{W}$ have to be located within a unit circle of the complex plane.

By using the mapping (16), the stability charts were calculated numerically in the parameter space of the control gains k_P, k_D, and the coupling term γ. Figure 2 shows the stability charts that correspond to the desired equilibrium $\boldsymbol{p}_0 = [0 \quad -1 \quad 0 \quad -1.5 \quad 0]^T$ and assume the realistic model parameters collected in Table 1. In addition, the sampling time of the applied controller was set to $\Delta t = 0.01$ s.

The series of charts in the upper panel of Fig. 2 show how the coupling parameter γ affect the stable domain of control parameters. When $\gamma = 1$ the coupling is removed and the cable connector oscillates, thus the plotted domain refers to marginal stability only. The enlarged charts in the lower panel present the inner structure of the stable domains at different, practically meaningful values of γ. It can be seen that the minimum spectral radii are almost the same in all the presented cases, however, when $\gamma = 0.8$ the fastest decaying transient can be achieved at low gains while the stable domain of control parameters is still sufficiently large. In these charts the different contour levels corresponds to the resolution 0.01 of the spectral radius.

In order to validate the results of the stability analysis and demonstrate the vibration attenuation of the investigated controller, the motion of the system was simulated with the nearly optimal gains $k_P = 100$ and $k_D = 12$, where the value of the corresponding spectral radius is $\rho = 0.94$ (see Fig. 2). In this simulation, the equilibrium state of the system was perturbed by changing the initial horizontal position of the cable connector to $x_2 = 0.05$ m. The resulting horizontal motions are presented by the solid lines in Fig. 3. During the numerical simulation the control forces were calculated according to Eq. (5). The integration was carried out by using the explicit 4th order Runge-Kutta method together with the projection method described in Ref. 13. The accuracy of the solution was provided via appropriate configuration correction and velocity filtering. The numerical solutions are compared to the semi-analytical solutions which are obtained via the evaluation of the linear mapping (16) with the same initial conditions. The solutions of the linearized system for the coordinates x_{CC} and x_{CU} are presented as dashed lines. These results are in good agreement with those obtained by the simulation of the original nonlinear equations subjected to geometric and control constraints.

In reality the actuators can have limitations. In case of the ACROBOTER platform, the applied thrust force is limited by the size of the built in ducted fans as well as the tolerable limit of the generated wind and noise. To capture the effect of actuator saturation the simulation were repeated by considering the maximum thrust force $\max(|F_T|) = 5$ N. Figures 4 and 5 show that applying only practically realizable control forces the violation of the servo-constraints are within an acceptable range and the attenuation of the vibrations of the perturbed system is sufficient. The detailed study of the nonlinear effect of the saturation is beyond the scope of the present paper, however, it is interesting to

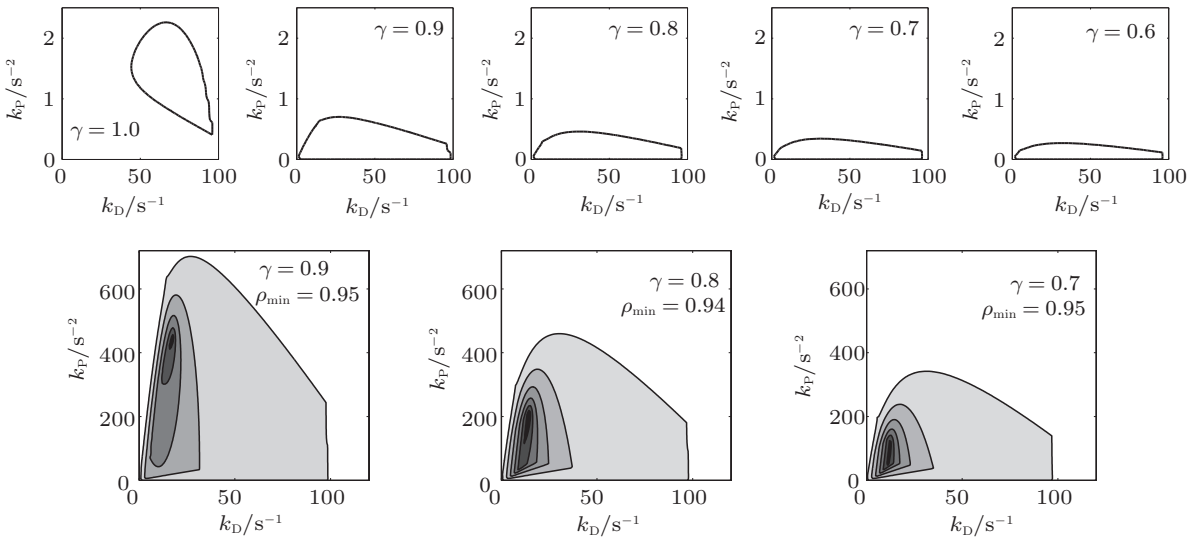

Fig. 2. Stability charts.

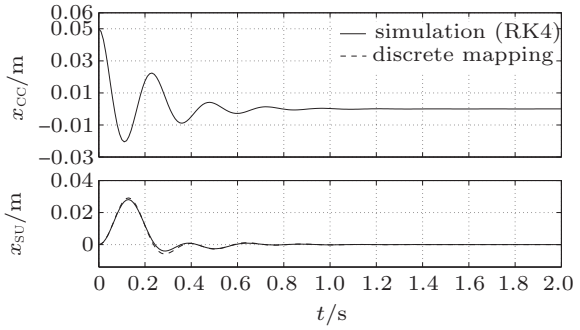

Fig. 3. Lateral vibrations of the CC and the SU.

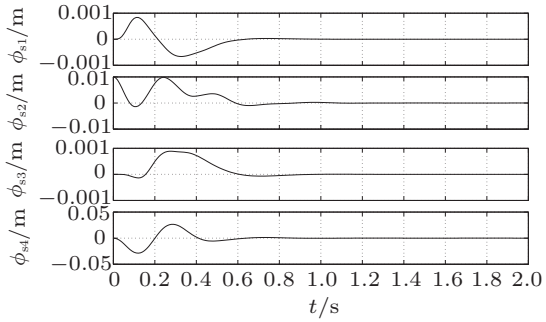

Fig. 5. Servo-constraint violations.

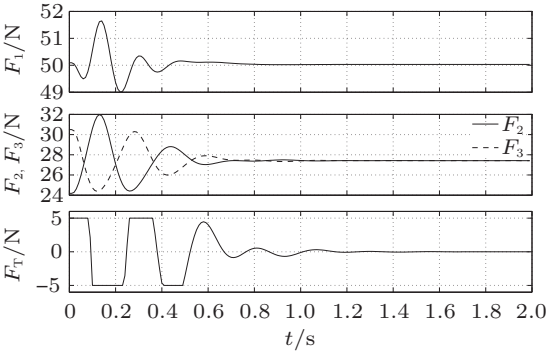

Fig. 4. Actuator forces.

note that it can be interpreted as a temporary and partial underactutaion of the corresponding actuator(s).

In this paper a computed torque control method was proposed for the control of the planar model of the ACROBOTER service robot. The method is based on the introduction of servo-constraints and it is applicable to calculate the actuator forces of a wide class of underactuated mechanical systems modeled by dependent coordinates. A real parameter case study was provided to select near optimal control gains for the control of the ACROBOTER robot. This selection is supported by stability charts that were obtained via the linearization of the investigated system around a desired equilibrium. The linearization was carried out by directly linearizing the DAE multibody equations and by applying an orthogonal projection in order to eliminate the Lagrangian multipliers associated with the constraint forces.

It can be concluded that the use of servo-constraints makes it possible to construct a PD controller that is realized via the stabilization of these constraints which enables the definition or modification of the applied controller in a relatively simple and intuitive way. A good example for this was the introduction of the coupling factor γ in the present paper.

Future work may include the elaboration of methods for the systematic design of the control parameters as well as the investigation of the effect of modifying the servo constraints such that the end effector of the robot must remain in a tube centered around the desired path. This interpretation of the actuator constraints would

result in larger position errors, but at the same time it could help to reduce/redistribute the loads on the different actuators.

This paper was presented at the 11th Conference on Dynamical Systems—Theory and Applications, December 5-8, 2011, Lodz, Poland.

1. J. Kövecses, IEEE/ASME Transactions on Mechatronics **8**, 165 (2003).
2. J. Jalón, and E. Bayo, *Kinematic and Dynamic Simulation of Multibody Systems: the Real-time Challenge* (Springer-Verlag, New York, 1994).
3. W. Blajer, and K. Kolodziejcyk, Multibody System Dynamics **11**, 343 (2004).
4. W. Blajer, and K. Kolodziejczyk, Journal of Theoretical and Applied Mechanics **46**, 383 (2008).
5. B. Siciliano, and O. Khatib, *Handbook of Robotics* (Springer-Verlag, Berlin, 2008).
6. I. Lammerts, *Adaptive Computed Reference Computed Torque Control of Flexible Manipulators* [Ph.D. thesis], Eindhoven University of Technology (1993).
7. L. Kovács, A. Zelei, and L. Bencsik, et al., Motion cortrol of and under-actuated servce robot using natural coordinates, in: W. S. Vincenzo ed, in: *Proceedings of Robot Design, Dynamics and Control*, (Wien, New York, 2010).
8. G. Stépán, and A. Toth, et al., *ACROBOTER: a ceiling based crawling, hoisting and swinging service robot platform*, in: Beyond Gray Droids: Domestic Robot Design for the 21st Century Workshop at Human Computer Interaction, (Cambridge, UK, 2009).
9. J. Baumgarte, Computer Methods in Applied Mechanics and Engineering **1**, 1 (1972).
10. W. Blajer, and K. Kolodziejczyk, Multibody System Dynamics **25**, 131 (2011).
11. J. Escalona, and R. Chamorro, Journal of Nonlinear Dynamics **53**, 237 (2008).
12. P. Masarati, Proceedings of the Institute of Mechanical Engineers, Part K: Journal of Multi-body Dynamics **223**, 335 (2009).
13. J. Kövecses, J. C. Piedoboeuf, and C. Lange, Journal of Applied Mechanics-Transactions of the ASME **75**, 12 (2008).
14. B. Minaker, and P. Frise, Journal of Vibration and Control **11**, 51 (2005).
15. R. DeCarlo, *Linear Systems: A State Variable Approach with Numerical Implementation* (Prentice Hall, New York, 1998).